

Low-temperature thermal and optical properties of single-grained decagonal Al-Ni-Co quasicrystals

A. D. Bianchi, F. Bommeli, E. Felder, M. Kenzelmann, M. A. Chernikov, L. Degiorgi, and H. R. Ott
Laboratorium für Festkörperphysik, Eidgenössische Technische Hochschule-Hönggerberg, CH-8093 Zürich, Switzerland

K. Edagawa

Institute of Industrial Science, University of Tokyo, Tokyo 106, Japan

(Received 25 November 1997; revised manuscript received 10 February 1998)

We report measurements of the specific heat $C_p(T)$ and of the thermal conductivities $\lambda^p(T)$ along the periodic direction and $\lambda^q(T)$ along a direction in the quasiperiodic plane for decagonal Al-Ni-Co at low temperatures. The coefficient $\gamma=0.63 \text{ mJ mol}^{-1} \text{ K}^{-2}$ of the linear term to $C_p(T)$ indicates a low density of electronic states at E_F . The magnitude of the cubic-in- T term to the low-temperature specific heat is in fair agreement with the acoustic contribution to $C_p(T)$ calculated from the results of low-temperature measurements of the elastic stiffness constants c_{ij} . The phonon contribution to $\lambda^p(T)$ shows a distinct maximum at 25 K, typical for periodic crystals. The dominant feature in the phonon contribution to $\lambda^q(T)$ is an extended plateau between 30 and 70 K, in agreement with the concept of generalized Umklapp processes in quasicrystals. This distinct difference between the phonon contributions to $\lambda^p(T)$ and $\lambda^q(T)$ is similar to that previously observed for $\text{Al}_{65}\text{Cu}_{20}\text{Co}_{15}$. The optical conductivity $\sigma_1(\omega)$ is obtained from reflectivity data in the frequency range between 1 meV and 12 eV. At low frequencies the optical conductivity $\sigma_1(\omega)$ is characterized by an anisotropic Drude contribution. At high frequencies an additional absorption for the periodic and the quasiperiodic direction is observed centered at approximately 1 and 2 eV, respectively, which can be associated with electronic excitations across a pseudogap. [S0163-1829(98)02230-9]

I. INTRODUCTION

The atomic arrangement in decagonal quasicrystals is periodic along the tenfold symmetry axis and quasiperiodic in the plane perpendicular to it. Thus, they share structural properties of periodically and quasiperiodically structured matter. The phase equilibria of the Al-Ni-Co alloy system allow the growth of large single-grained decagonal quasicrystals,¹ crucial in studying reliably anisotropic properties. For decagonal quasicrystals in the Al-Cu-Co and Al-Ni-Co systems, strong anisotropies of electrical^{2,3} and thermal transport⁴⁻⁶ as well as the optical conductivity⁷ have been established experimentally. The values of the residual electrical resistivity ρ observed in decagonal quasicrystals along the periodic ρ_0^p and along the quasiperiodic direction ρ_0^q show an anisotropy ρ_0^p/ρ_0^q of the order of 10. However, $\rho^p(T)$ as well as $\rho^q(T)$ change only little with temperature.

Measurements of the thermal conductivity $\lambda(T)$ of decagonal Al-Cu-Co showed that the phonon contributions to $\lambda(T)$ along the periodic direction $\lambda_{\text{ph}}^p(T)$ and along a direction in the quasiperiodic plane $\lambda_{\text{ph}}^q(T)$ are qualitatively different.⁵ While the thermal conductivity via lattice excitations along the periodic direction $\lambda_{\text{ph}}^p(T)$ showed a distinct maximum centered at 25 K, the thermal conductivity $\lambda_{\text{ph}}^q(T)$ along a direction in the quasiperiodic plane turned out to be almost temperature independent above 30 K. These results gave further evidence for the differing characteristics of Umklapp scattering of lattice excitations in solids with periodic⁸ and quasiperiodic orders,⁹ which are believed to be a direct consequence of the difference between the lattice excitation

spectra of periodic and quasiperiodic lattices. In a periodic crystal, the exponential decrease with decreasing temperature of high frequency phonons available for Umklapp processes leads to an exponential decrease of the Umklapp scattering rate of the phonons. In a quasicrystal the situation is apparently different, because the momentum of vibrational excitations can be transferred to the quasilattice in inelastic scattering events by arbitrarily small portions, i.e., not limited in magnitude from below, resulting in a power-law decrease of the rate of Umklapp processes.

A theoretical investigation on the lattice dynamics of a high-order periodic approximant of decagonal Al-Mn indicated a strongly anisotropic phonon dispersion relation and the presence of a hierarchy of optical excitations down to very low energies, located at the boundaries of the pseudo-Brillouin zone.¹⁰

Optical properties of icosahedral quasicrystals differ from those of either metals or semiconductors.¹¹⁻¹³ A common feature in the charge dynamic spectrum of icosahedral quasicrystals, e.g., in the Al-Mn-Pd and Al-Re-Pd systems, expressed in terms of the real part $\sigma_1(\omega)$ of the complex optical conductivity $\sigma(\omega)$, is the large absorption in the visible spectral range. This absorption is usually ascribed to excitations across a pseudogap in the electronic excitation spectrum that is thought to open due to the Hume-Rothery-type stabilization of an icosahedral phase.¹¹⁻¹³ Below the visible spectral range, another broad absorption in $\sigma_1(\omega)$, extending from mid infrared (MIR) down to far infrared (FIR) is observed. Its origin is still quite puzzling. While first reports on optical investigations^{11,12} claim that this absorption is due to a mobility-gap feature, more recent and comprehensive stud-

ies, combining electrical, magnetic, and optical data,¹⁴ seem to seriously question and, in fact, invalidate that interpretation. The broad low-frequency tail in $\sigma_1(\omega)$ below 0.4 eV is rather to be ascribed to a distribution of bound states.¹⁴ Another relevant issue that still remains unresolved, is to what extent the unusual behavior of $\sigma_1(\omega)$ in icosahedral quasicrystals should specifically be attributed to the quasiperiodic long-range order. Important information on the electrodynamic response of quasiperiodically structured solids can be obtained using decagonal quasicrystals, which offer a unique opportunity for a *comparative* study of optical properties of both periodically and quasiperiodically structured matter using light that is linearly polarized along different crystallographic directions of one single sample.

Here we report results of measurements of the low-temperature specific heat $C_p(T)$ and the thermal conductivities $\lambda^p(T)$ and $\lambda^q(T)$ along the periodic direction and along a direction in the quasiperiodic plane, respectively, for high-quality single-grain samples of decagonal Al-Ni-Co in varying temperature ranges between 0.07 and 80 K. The specific heat data provide additional information for establishing the low-frequency lattice dynamics and vibrational density of states, complementary to results obtained in inelastic neutron scattering experiments.¹⁵

In addition to our thermal-transport and thermodynamic investigations of decagonal Al-Ni-Co and in order to reach a comprehensive understanding of decagonally structured solids, we also aim at mapping the complete electronic excitation spectrum. Optical investigations, performed over a very broad range of frequencies, have proven to be very useful for identifying the spectrum of excitations. An analysis of the complete electrodynamic response allows one to evaluate the plasma frequency ω_p and the scattering rate Γ of the free charge carriers contribution, and also parameters characterizing electronic transitions and optically active lattice excitations.

This set of data substantially extends the temperature range of previous investigations of the specific heat¹⁶ and thermal transport^{4,6} in Al-Ni-Co. In addition, to the best of our knowledge, information on the optical properties of decagonal Al-Ni-Co has not been obtained.

II. SAMPLES AND EXPERIMENT

Al-Ni-Co quasicrystals were grown using the self-flux technique. An $\text{Al}_{70}\text{Co}_{15}\text{Ni}_{15}$ alloy was prepared by arc melting using high-purity elemental metals (99.999 % pure aluminum, 99.9985 % pure nickel, and 99.997 % pure cobalt). The resulting button was loaded in an alumina crucible and sealed under vacuum in a silica ampoule. The ingot was remelted at 1250 °C, cooled to 1030 °C at a rate of 2 °C per h, annealed at 1030 °C for 5 days, and subsequently rapidly cooled to room temperature. The resulting ingot contained several large grains with decaprismatic morphology, partly embedded in the bulk of the material. Samples were cut from the decaprisms using a spark cutter. Two samples cut perpendicular and parallel to the decagonal (periodic) axis A_{10} with approximate dimensions $4 \times 2.2 \times 1.7 \text{ mm}^3$ and $2.4 \times 2.1 \times 1.5 \text{ mm}^3$ were selected for our experiments. No grain boundaries were observed in a scanning electron microscope analysis. An electron-diffraction experiment revealed that

these samples are highly ordered quasicrystals with a very small phason strain and with the $S1$ superstructure type of decagonal order, indicating that the most probable chemical composition of the samples is $\text{Al}_{71}\text{Ni}_{16}\text{Co}_{13}$.¹⁷ Laue photographs taken on both samples have confirmed that they are single quasicrystals.

The larger sample was used for measurements of the thermal conductivity $\lambda^p(T)$ along the decagonal axis. The smaller sample was used for measurements of the thermal conductivity $\lambda^q(T)$ along a direction in the quasiperiodic plane, of the specific heat $C_p(T)$ and of the optical reflectivity $R(\omega)$. Subsequently this sample was also used for resonant ultrasound spectroscopy experiments.¹⁸

The thermal conductivity $\lambda(T)$ was measured using a standard steady-state heat-flow technique monitoring the temperature gradient along the sample. The specific heat $C_p(T)$ was measured using a conventional relaxation-type method. The temperatures in the range between 0.06 and 1 K were reached using a dilution refrigerator. Conventional ³He and ⁴He cryostats were used for temperatures between 0.35 and 3 K, and above 1.5 K, respectively.

The optical reflectivity $R(\omega)$ of decagonal $\text{Al}_{71}\text{Ni}_{16}\text{Co}_{13}$ was measured in the frequency range between 1 meV and 12 eV, i.e., over more than four orders of magnitude in frequency and at selected fixed temperatures. The reflectivity $R(\omega)$ was obtained both from the surface parallel to the quasiperiodic plane and from the surface parallel to the decagonal axis. In the latter experiment linearly polarized light was used with the electric field vector \mathbf{E} direction either parallel or perpendicular to the decagonal axis.

Four spectrometers with overlapping frequency ranges were used.^{13,14} In the far infrared we made use of a Bruker IFS 113 v Fourier interferometer with a Hg arc-light source and He-cooled Ge-bolometer detector, while from the FIR up to the MIR range a fast scanning Bruker interferometer IFS48PC was used. In the visible spectral range a home-made spectrometer based on a Zeiss monochromator was employed and in the ultraviolet we used a McPherson spectrometer. From the MIR down to the FIR we used the reflectivity of tungsten as a reference.

The complete set of optical properties, i.e., the complex optical conductivity $\sigma(\omega) = \sigma_1(\omega) + i\sigma_2(\omega)$ was obtained via a Kramers-Kronig transformation of the reflectivity $R(\omega)$ spectra extrapolated to lower and higher frequencies. To this end, $R(\omega)$ was extrapolated to lower frequencies using the Hagen-Rubens relation $1 - R(\omega) \propto \sqrt{\omega}$, i.e., assuming a metallic behavior. Above the highest frequency achieved in this experiment, we first used the extrapolation $R \propto 1/\omega^2$, which is meant to simulate the reflectance in the frequency range of interband transitions, and at frequencies higher than 40 eV, we assumed $R \propto 1/\omega^4$, simulating the behavior of free electrons.^{13,14}

III. RESULTS AND ANALYSIS

A. Specific heat

The complete set of the specific heat $C_p(T)$ data in the temperature range between 1.5 and 36 K for a single grain of decagonal Al-Ni-Co is shown on a double logarithmic plot in Fig. 1. The same data in the form of C_p/T vs T^2 , are plotted

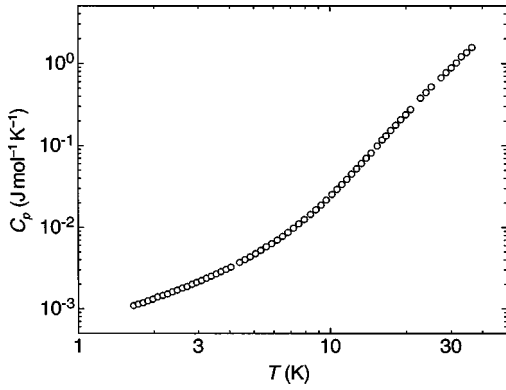


FIG. 1. Specific heat $C_p(T)$ of decagonal $\text{Al}_{71}\text{Ni}_{16}\text{Co}_{13}$ between 1.5 and 36 K.

in Fig. 2. Between 1.5 and 3 K the temperature variation of $C_{\text{ph}}(T)$ can adequately be described by assuming that the main contributions are due to electronic and lattice excitations, i.e.,

$$C_p(T) = \gamma T + \beta T^3. \quad (1)$$

A fit of Eq. (1) to our specific-heat data $C_p(T)$ using Eq. (1), which is shown in Fig. 2 as the solid line, yields $\gamma = 0.629 \pm 0.003 \text{ mJ mol}^{-1} \text{ K}^{-2}$ and $\beta = 9.5 \pm 0.6 \text{ } \mu\text{J mol}^{-1} \text{ K}^{-4}$, corresponding to a Debye temperature Θ_D of $589 \pm 12 \text{ K}$. For calculating Θ_D the experimentally determined density $\rho = 4.186 \text{ g cm}^{-3}$ was used.¹⁸ We note that the measured value of ρ for $\text{Al}_{71}\text{Ni}_{16}\text{Co}_{13}$ is distinctly lower than the averaged density of the constituent elemental metals. Our value of the parameter γ reported here is close to analogous values reported previously for melt-spun $\text{Al}_{70}\text{Ni}_{30-x}\text{Co}_x$ ribbons, with $5 < x < 30$.¹⁶ This value of the electronic specific heat parameter γ is 2.5 times smaller than that of aluminum but somewhat higher than the γ values previously reported for highly ordered icosahedral Al-Mn-Pd and Al-Re-Pd quasicrystals with the face centered icosahedral structure, which fall into the range between 0.11 and $0.41 \text{ mJ mol}^{-1} \text{ K}^{-2}$.^{14,19} For these materials, the small electronic specific heat has tentatively been attributed to the presence of a pseudogap in the density of electronic states (DOS) at the Fermi energy E_F .^{14,19} Subsequent optical reflectivity measurements using the same samples gave further evidence supporting this

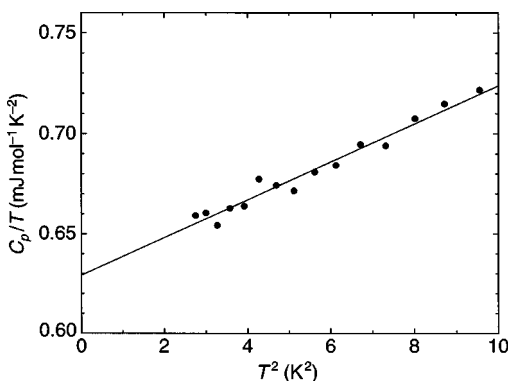


FIG. 2. Specific heat of decagonal $\text{Al}_{71}\text{Ni}_{16}\text{Co}_{13}$ plotted as C_p/T vs T^2 . The solid line is the fit to the data using Eq. (1) in the temperature range between 1.5 and 3 K.

conclusion.^{13,14} The pseudogap in the electronic DOS at E_F of icosahedral quasicrystals in the Al-Mn-Pd, Al-Re-Pd, and Al-Cu-Fe alloy systems was also inferred from an analysis of the low-temperature high-resolution ultraviolet photoemission spectra.²⁰

Calculations of the electronic band structure for periodic approximants in the Al-Cu-Fe (Ref. 21) and Al-Mn-Pd (Ref. 22) systems indicated the existence of a well pronounced pseudogap at the Fermi energy E_F . In the Al-Mn-Pd system the calculated electronic DOS of a series of approximants indicated that the position of the pseudogap relative to E_F is influenced by changes in the chemical composition.²² It was found that for higher-order approximants the minimum in the electronic DOS is located closer to E_F ,²² however, the depth of the pseudogap is almost independent of the order of the approximant.²² In the same work the importance of the hybridization of the Al s and p states with the transition metal d states in the formation of the pseudogap was pointed out as a result of a calculation of the electronic DOS of a series of clusters.²² A calculation of the electronic band structure in periodic Al-based Hume-Rothery alloys lead to a similar conclusion.²³ The results of these band structure calculations gave evidence for the validity of a model assuming an enhanced formation of a pseudogap in the electronic DOS at E_F by the combination of the crossing of a d with an sp band at the pseudo-Brillouin zone boundary.²⁴

While abundant experimental evidence for the existence of a pronounced pseudogap in the density of electronic states at E_F has experimentally been obtained for various icosahedral phases,²⁵ suggesting that the Hume-Rothery mechanism plays an essential role in the stability of the icosahedrally ordered solids,^{26,24} the presence of a pseudogap at E_F in decagonal quasicrystals remains a controversial issue. We thus briefly discuss some experimental and theoretical aspects related to this matter. The results of Hall-effect measurements reported in Ref. 27 seem to support the Hume-Rothery-type scenario. The low linear-in- T contribution to C_p of decagonal Al-Cu-Co (Ref. 5) and Al-Ni-Co indicate a reduced DOS at E_F in decagonal quasicrystals. Based on the analysis of high-resolution photoemission experiments, the presence of a pseudogap in decagonal Al-Cu-Co and Al-Ni-Co was claimed by Stadnik and co-workers.²⁸

The absence of a pseudogap at E_F in the electronic density of states in decagonal $\text{Al}_{62}\text{Co}_{15}\text{Cu}_{20}\text{Si}_3$ and $\text{Al}_{65}\text{Co}_{17}\text{Cu}_{18}$ has been inferred from an analysis of the optical conductivity $\sigma_1(\omega)$, which indicated a higher density of free charge carriers n in these systems compared with the values of n observed in icosahedral quasicrystals.⁷ Nevertheless, our results on $\sigma_1(\omega)$ in decagonal Al-Ni-Co presented here clearly show an absorption centered at approximately 1 eV for both directions. Such an absorption is a general observation in the $\sigma_1(\omega)$ curves of icosahedral quasicrystals and is commonly associated with excitations across a pseudogap in the electronic excitation spectrum. This point will be discussed in more detail in Sec. III C. Calculations of the electronic band structure of rational approximants to decagonal quasicrystals have raised some doubts as to whether the observed minimum in the electronic DOS of decagonal quasicrystals is due to an electronically driven stabilization of quasiperiodic structures.^{29,30}

A recent band structure calculation using a model approximant $\text{Al}_{66}\text{Cu}_{30}\text{Co}_{14}$ of decagonal Al-Cu-Co showed the presence of a pseudogap with a width of ≈ 0.5 eV centered at an energy of ≈ 0.3 eV above E_F .³¹ The overall energy dependence of the electronic DOS is, however, in poor agreement with the photoelectron spectra reported for a decagonal quasicrystal of a somewhat different chemical composition.^{28,30} In addition, it turned out that both the position and the depth of the pseudogap in the calculated electronic DOS of decagonal Al-Cu-Co strongly depend on the chemical decoration of the Cu/Co sites.^{29,30} For certain decorations of the Cu/Co sites, the minimum in the partial DOS of the Al s and p states near E_F is covered by the large contribution from the Co d states.³⁰ These observations have led to the conclusion that a pseudogap in the electronic DOS of decagonal Al-Cu-Co is the consequence of the hybridization between transition metal d states and aluminum s and p states rather than the result of the interaction of the Fermi surface with the pseudo-Brillouin zone.^{29,30} A similar conclusion regarding the origin of the pseudogap at E_F in decagonal quasicrystals has emerged from electronic band structure calculations for decagonal Al-Mn-Pd.³² Concluding this discussion, we note that our results on the low-temperature specific heat indicate a small electronic DOS at E_F and are therefore consistent with the presence of a pseudogap in the electronic DOS at E_F .

We now concentrate on the lattice contribution $C_{\text{ph}}(T)$ to the specific heat C_p of decagonal Al-Ni-Co. The specific heat data plotted in Fig. 2 as C_p/T vs T^2 falls on a straight line, indicating a Debye-type behavior of $C_{\text{ph}}(T)$ for temperatures below 3 K. At low temperatures only the acoustic excitations contribute to $C_{\text{ph}}(T)$, which takes the form

$$C_D(T) = \frac{2\pi^2 k_B^4}{5\hbar^3 v_s^3} T^3, \quad (2)$$

where $1/v_s^3$ is the average of the inverse third power of the long-wavelength phase velocities $v_i(\mathbf{q})$ of the three acoustic modes:

$$\frac{1}{v_s^3} = \frac{1}{3} \sum_{i=1}^3 \int \frac{1}{v_i^3(\varphi, \theta)} \frac{d\varphi \sin\theta d\theta}{4\pi}. \quad (3)$$

Here $v_i(\varphi, \theta)$ are the velocities of the sound waves propagating in a direction defined by the directional angles φ and θ . From the low-temperature values of the elastic moduli c_{ij} obtained using resonant ultrasound spectroscopy¹⁸ and the measured mass density ρ we deduce the average sound velocity v_s to be $(4.910 \pm 0.02) \times 10^3$ m/s. This value, inserted into Eq. (2), gives a low-temperature contribution to the specific heat of $C_D(T) = (8.93 \pm 0.11) T^3 \mu\text{J mol}^{-1} \text{K}^{-1}$, in fair agreement with the abovementioned experimental result $\beta T^3 = (9.5 \pm 0.6) T^3 \mu\text{J mol}^{-1} \text{K}^{-1}$. This is quite different than the situation in icosahedral quasicrystals, for which a large excess cubic-in- T term in the low-temperature specific heat $C_p(T)$ has previously been observed in the Al-Mn-Pd and Al-Re-Pd systems.³³

The lattice specific heat $C_{\text{ph}}(T)$ obtained by subtracting off the linear contribution γT from the measured specific heat $C_p(T)$ is shown as a plot of C_{ph}/T^3 vs T in Fig. 3. As

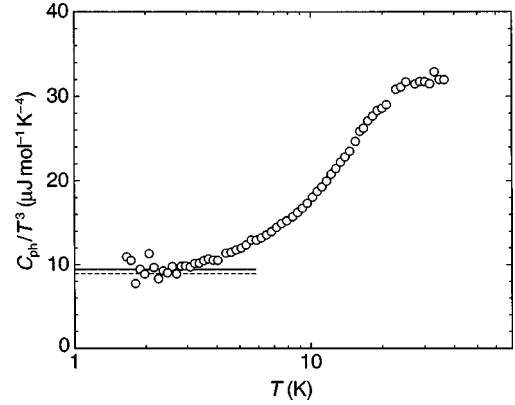


FIG. 3. The lattice specific heat is plotted as C_{ph}/T^3 vs T . The solid line shows the result of the fit to Eq. (1), with $C_{\text{ph}}/T^3 = 9.5 \mu\text{J mol}^{-1} \text{K}^{-4}$. The dashed line is the the long-wavelength acoustic contribution to the specific heat $C_D/T^3 = 8.93 \mu\text{J mol}^{-1} \text{K}^{-4}$ (see text).

noted above, the C_{ph}/T^3 ratio is temperature independent below 3 K. For temperatures higher than 3 K, the C_{ph}/T^3 ratio increases rapidly with increasing temperature above the constant Debye limit, indicating that with increasing ω the vibrational DOS $g(\omega)$ increases more strongly than the Debye approximation

$$g(\omega) = \frac{3}{2\pi^2 v_s^3} \omega^2. \quad (4)$$

With further increasing temperature, C_{ph}/T^3 tends to saturate above 30 K at the level of $32 \mu\text{J mol}^{-1} \text{K}^{-4}$, approximately a factor of 3 higher than the ratio C_D/T^3 . At high temperatures $T > \Theta_D$ the lattice specific heat $C_{\text{ph}}(T)$ is expected to reach the constant Dulong-Petit limit and therefore C_{ph}/T^3 vs T passes through a maximum at intermediate temperatures. This trend to saturation of the C_{ph}/T^3 vs T curve simply indicates the proximity to this maximum.

In the harmonic approximation, the lattice specific heat $C_{\text{ph}}(T)$ depends on the DOS $g(\omega)$:

$$C_{\text{ph}}(T) = \int_0^\infty g(\omega) \frac{\partial}{\partial T} \left(\frac{\hbar \omega}{\exp(\hbar \omega / k_B T) - 1} \right) d\omega. \quad (5)$$

The phonon DOS $g(\omega)$ cannot, strictly speaking, unambiguously be determined from the measured lattice specific heat $C_{\text{ph}}(T)$, as this requires solving an integral equation with an unstable kernel.³⁴ An analysis of the $C_{\text{ph}}(T)$ behavior may nevertheless provide relevant information on $g(\omega)$, because the integral in Eq. (5) is especially sensitive to the variation of $g(\omega)$ close to $\omega \approx 2.3k_B T/\hbar$. The information on $g(\omega)$ obtained from the $C_{\text{ph}}(T)$ analysis is particularly accurate in the low-frequency limit, in which the contribution from high-frequency modes is exponentially small.

The increase of $C_{\text{ph}}(T)$ with increasing temperature above the Debye limit may be related to either low-lying optical modes or the dispersion of acoustical excitations. In decagonal $\text{Al}_{71}\text{Ni}_{16}\text{Co}_{13}$ the presence of an optical branch at the frequency $\omega = 1.9 \times 10^{13}$ rad/s may be inferred from the splitting of the $\omega(\mathbf{q})$ data for transverse excitations measured using inelastic neutron scattering along the $(1, 1, -1, 0)$

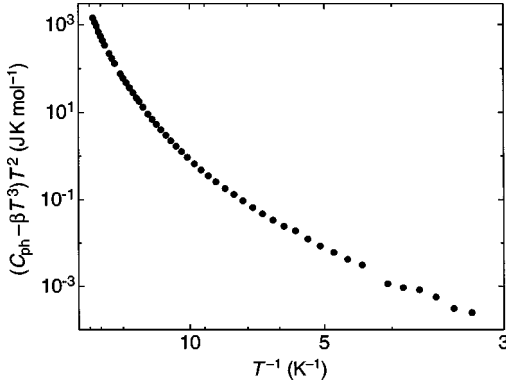


FIG. 4. $(C_{\text{ph}} - \beta T^3)T^2$ vs T^{-1} plotted on a semilogarithmic scale.

crystallographic direction.³⁵ Theoretical calculations of the vibrational DOS using the modified Burkov model³⁶ suggest the presence of an optical mode in the frequency range between 1.5×10^{13} and 2.4×10^{13} rad/s.³⁷ However, no optical mode in this frequency range was resolved in the generalized vibrational density of states (GVDOS) of quasicrystalline Al-Ni-Co as determined by time-of-flight inelastic neutron scattering.³⁷

In Fig. 4 we show the difference between C_{ph} and βT^3 multiplied by T^2 as function of the inverse temperature on a semilogarithmic plot. The $(C_{\text{ph}} - \beta T^3)T^2$ data do not fall on a straight line indicating that a singular low-frequency optical branch can be ruled out as the origin of the observed $C_{\text{ph}} - \beta T^3$. This is because at temperatures $T \ll \hbar \omega_0 / k_B$ a singular optical excitation with an energy $\hbar \omega_0$ is expected to contribute a term to the specific heat that increases exponentially with increasing temperature [Eq. (5)]. We note that below 8 K $C_{\text{ph}} - \beta T^3$ displays rather a power-law behavior, as can be seen on the double logarithmic plot of $C_{\text{ph}} - \beta T^3$ vs T in Fig. 5. The solid line in Fig. 5 is compatible with $C_{\text{ph}} - \beta T^3 \propto T^n$ and $n = 5.1 \pm 0.1$. Approximating $C_{\text{ph}} - \beta T^3$ by δT^n with $n = 5$, we obtain $\delta = 96 \pm 0.2$ nJ mol⁻¹ K⁻⁶. A T^5 term in the lattice specific $C_{\text{ph}}(T)$ may have its origin in a ω^4 term in the vibrational density of states $g(\omega)$ indicating the dispersion of acoustic excitations.

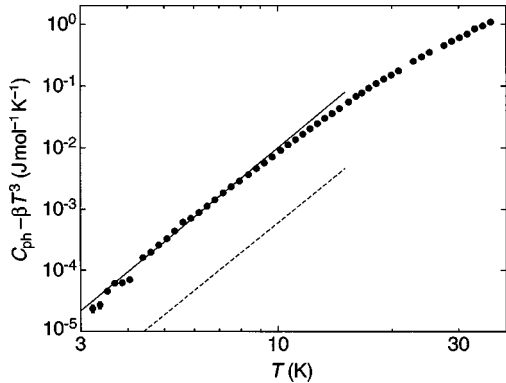


FIG. 5. $C_{\text{ph}} - \beta T^3$ vs T plotted on logarithmic scales. The solid line indicates a fit to a power law $C_{\text{ph}} - \beta T^3 \propto T^5$. The dashed line is an estimate of the T^5 contribution to $C_p(T)$ which is compatible with the experimentally determined values of the phonon dispersion relations $\omega(\mathbf{q})$ for decagonal Al-Ni-Co (see text).

TABLE I. Parameters of the fit of the phonon dispersion $\omega(\mathbf{q})$ data of decagonal Al-Ni-Co in the range $|\mathbf{q}| < 0.55$ Å using Eq. (6).

Direction	v_l (m/s)	α_l $\times 10^{-17}$ (m ³ /s)	v_t (m/s)	α_t $\times 10^{-17}$ (m ³ /s)
(0,0,0,2)	7490 ± 120	-5.8 ± 0.6	3990 ± 60	-1.7 ± 0.4
(1,1,-1,-1,0)	7900 ± 500	-8 ± 2	4060 ± 60	-1.3 ± 0.4

The dispersion relation of acoustic excitations $\omega(\mathbf{q})$ can be expanded in a power series of the form

$$\omega_i(\mathbf{q}) = v_i q + \alpha_i q^3 + \mathcal{O}(q^5), \quad i = l, t_1, t_2. \quad (6)$$

The phonon dispersion $\omega(\mathbf{q})$ in Al₇₁Ni₁₆Co₁₃ has been determined at 300 K by inelastic neutron scattering using a triple axis spectrometer.³⁵ Two transversal and two longitudinal modes were observed starting close to the Bragg peaks at (0,0,0,2) and (1,1,-1,-1,0) and propagating parallel to the (1,1,-1,-1,0) and (0,0,0,2), crystallographic directions, respectively.³⁵ The polarization vectors of these modes were lying in the plane defined by the (0,0,0,2) and (1,1,-1,-1,0) directions.³⁵ The parameters v_i and α_i of a fit of Eq. (6) to the $\omega(\mathbf{q})$ data in the wave vector range $|\mathbf{q}| < 0.55$ Å are given in Table I. We note that the v_i determined from the fits to the $\omega(\mathbf{q})$ data are in good agreement with the sound velocities obtained from the measured low-temperature elastic stiffness constants c_{ij} .¹⁸ The observed phonon dispersion was found to be isotropic within the experimental errors for $|\mathbf{q}| < 0.55$ Å. This is again in agreement with the results of the resonant ultrasound spectroscopy experiment¹⁸ indicating that the variation of the sound velocities with the angle θ between the wave vector and the decagonal axis is 13% at most. These experimental findings are quite in contrast to the results of a theoretical investigation of lattice excitations in decagonal Al-Mn, suggesting a strongly anisotropic dispersion for lattice excitations propagating in the quasiperiodic plane and along the periodic direction.¹⁰

A crude estimate of $g_4(\omega)$ may be obtained assuming that the phonon dispersion in decagonal Al-Ni-Co is isotropic at low $|\mathbf{q}|$ and that the transverse acoustical branch is doubly degenerate. This assumption leads to the vibrational density of states $g_4(\omega)$ of the form

$$g_4(\omega) = -\frac{5}{2\pi^2} \left(\frac{\alpha_l}{v_l^6} + 2 \frac{\alpha_t}{v_t^6} \right) \omega^4. \quad (7)$$

Substituting this result into Eq. (5) gives

$$C_{\text{ex}}(T) = -\frac{40\pi^4 k_B^6}{21\hbar^5} \left(\frac{\alpha_l}{v_l^6} + 2 \frac{\alpha_t}{v_t^6} \right) T^5. \quad (8)$$

Using the values of v_l , v_t , α_l , and α_t given in Table I, leads to $C_{\text{ex}}/T^5 = 6$ nJ mol⁻¹ K⁻⁶. This value is 15 times smaller than the experimentally determined coefficient of the T^5 term to the specific heat $C_p(T)$. Thus the dispersion of acoustical excitations in decagonal Al-Ni-Co cannot account for the observed deviation from the Debye-type behavior of the low-temperature lattice specific heat $C_{\text{ph}}(T)$. Given the

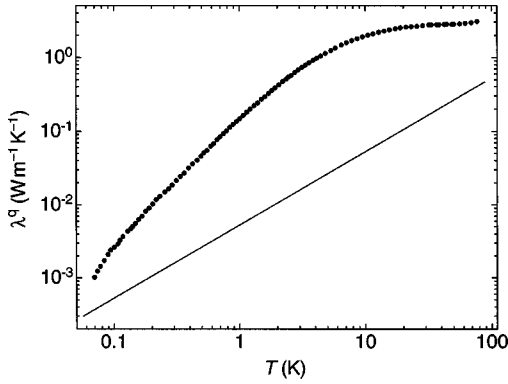


FIG. 6. The total measured thermal conductivity λ^q of decagonal $\text{Al}_{71}\text{Ni}_{16}\text{Co}_{13}$ in a quasiperiodic direction between 0.06 and 80 K. The solid line is an estimate of the electronic contribution λ_{el}^q (see text).

small degree of polar elastic anisotropy in decagonal Al-Ni-Co as revealed by ultrasound resonant spectroscopy¹⁸ and inelastic neutron scattering,³⁵ it seems quite unlikely, that a stronger curvature of the phonon dispersion $\omega(\mathbf{q})$ along certain directions in the reciprocal space than that already measured is the cause of the observed deviation of $C_{\text{ph}}(T)$ from a Debye-type behavior. But unless $\omega(\mathbf{q})$ has been measured along additional directions in reciprocal space this possibility cannot be ruled out completely. Another possible explanation of this discrepancy could be a distribution of nonpropagating lattice excitations with a density $g(\omega) \propto \omega^4$. However, at present we are not aware of any theoretical model featuring such a behavior.

B. Thermal conductivity

1. Quasiperiodic direction

The thermal conductivity λ^q of Al-Ni-Co along a direction in the quasiperiodic plane in the temperature range between 0.06 and 80 K is shown on double logarithmic scales in Fig. 6. The solid line is an estimate of the electronic contribution λ_{el}^q , which was calculated from electrical resistivity ρ^q data measured on this same sample and assuming the validity of the Wiedemann-Franz law.

The lattice contribution $\lambda_{\text{ph}}^q(T)$, obtained by subtracting $\lambda_{\text{el}}^q(T)$ from the measured thermal conductivity $\lambda^q(T)$, is shown in Fig. 7. It increases considerably with increasing T between 0.07 and 2 K. With further increasing of T , we note the trend of $\lambda_{\text{ph}}^q(T)$ to saturate at 30 K and from 30 to 80 K λ_{ph}^q is almost temperature independent. The occurrence of a plateau-type feature in the thermal conductivity $\lambda_{\text{ph}}^q(T)$ of decagonal Al-Ni-Co along a direction in the quasiperiodic plane is compatible with theoretical expectations considering generalized Umklapp processes in solids with quasiperiodic order.⁹ Those are based on the argument that for a quasicrystal one expects a hierarchy of gaps in the vibrational excitation spectrum $\omega(\mathbf{q})$ at any frequency less than the maximum lattice frequency ω_{max} . For quasiperiodic lattices, the gaps due to the Bragg peaks at small k and therefore small frequency transfers ω of the back-scattered acoustical waves, may provide a substantial contribution to the probability of Umklapp processes of the phonons, even if the gap widths

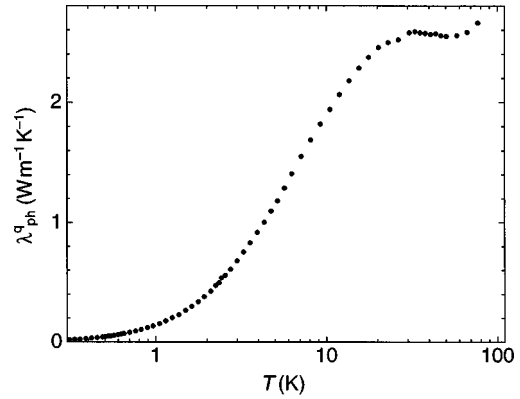


FIG. 7. The lattice contribution λ_{ph}^q along a direction in the quasiperiodic plane obtained by subtracting λ_{el}^q from λ^q , shown on a semilogarithmic scale.

are small. As a result, the rate of the generalized Umklapp processes in quasicrystals has a weak power-law dependence, reflecting the fact that the momentum of vibrational excitations can be transferred to the quasilattice in inelastic scattering events by arbitrarily small portions, i.e., not limited in magnitude from below.⁹ This is quite in contrast to periodic crystals, for which the rate of the Umklapp processes shows an exponential temperature dependence.⁸ The weak temperature dependence of the phonon scattering rate in quasicrystals is expected to lead to a shallow maximum or even to a plateau in the $\lambda_{\text{ph}}^q(T)$ curve (see Fig. 7). The plateau-type feature in the phonon thermal conductivity curve $\lambda_{\text{ph}}^q(T)$ seems to be a general observation for quasicrystals^{38–41} and it has previously been observed for decagonal Al-Cu-Co along the quasiperiodic direction⁵ as well as for icosahedral Al-Mn-Pd, Al-Cu-Fe, and Al-Re-Pd.

2. Periodic direction

In Fig. 8 we show the thermal conductivity λ^p measured along the periodic direction in the temperature range between 0.45 and 80 K plotted on logarithmic scales. We estimate the electronic contribution λ_{el}^p to λ^p by assuming that $\lambda^p(T)$ high and low temperatures is dominated by λ_{el}^p given by the law of Wiedemann and Franz, which is justified by

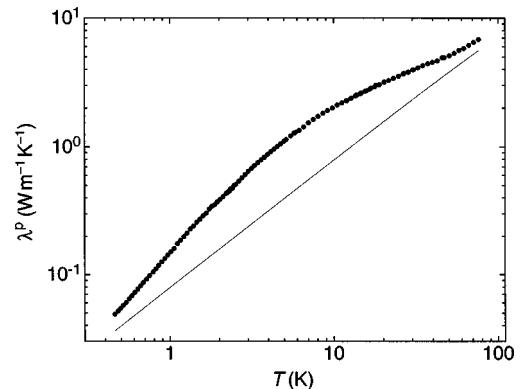


FIG. 8. Temperature dependence of the total thermal conductivity λ^p along the periodic direction of decagonal $\text{Al}_{71}\text{Ni}_{16}\text{Co}_{13}$ between 0.45 and 80 K. The solid line is an estimate of the electronic contribution λ_{el}^p , as explained in the text.

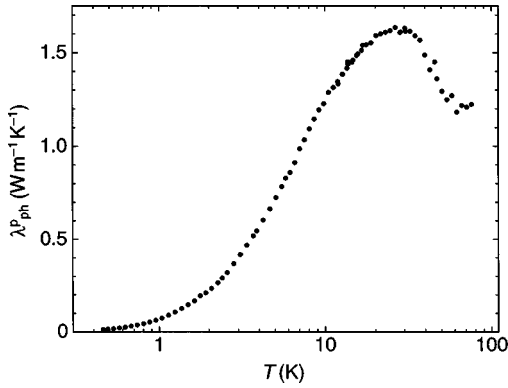


FIG. 9. Phonon contribution λ_{ph}^p to the thermal conductivity along the periodic direction.

comparison with the situation for Al-Cu-Co.⁵ The result of this calculation is shown as the solid line in Fig. 8.

The lattice contribution λ_{ph}^p , obtained by subtracting λ_{el}^p from the measured thermal conductivity λ^p , is shown in Fig. 9. At 25 K, $\lambda_{\text{ph}}^p(T)$ passes over a maximum and decreases distinctly with further increasing T . This behavior is reminiscent of that of periodic crystals, where $\lambda_{\text{ph}}(T)$ at intermediate temperatures (10–30 K) is characterized by a crossover from the regime of boundary-limited or phonon-electron scattering and to the regime of increasing Umklapp phonon scattering.

In periodic crystals, in the temperature region just above that maximum, the phonon thermal resistance is dominated by the onset of Umklapp processes. In this regime, λ_{ph} is expected to decrease exponentially with increasing temperature due to an exponential increase of the occupation number of the phonon modes with frequencies high enough to allow the occurrence of Umklapp processes, i.e., of the order of the Debye frequency.⁸ While above the maximum a decrease of λ_{ph}^p with increasing temperature is observed (see Fig. 9), it is, however, not possible to identify the exponential dependence. In this connection we note that even in single crystals the exponential variation of $\lambda_{\text{ph}}^p(T)$ is most often masked by isotope or impurity scattering effects.⁴² Nevertheless, even in polycrystalline or impure samples a distinct maximum of $\lambda_{\text{ph}}(T)$ is observed. Far below the temperature at which the maximum in the $\lambda_{\text{ph}}(T)$ occurs, the phonon mean free path in periodic crystals is limited either by sample-boundary scattering (in insulators) or by phonon-electron scattering (in metals). Both these mechanisms result in a positive slope of the λ_{ph} curve. A crossover from the regime of Umklapp scattering at high temperatures and the regime of either boundary or electron-phonon scattering at low temperatures results necessarily in a maximum in the λ_{ph} vs T curve.

Between 0.45 and 1.2 K, the phonon thermal conductivity is well described by $\lambda_{\text{ph}}^p \propto T^n$, where $n = 2.2 \pm 0.1$ (see solid line in Fig. 10). An approximately quadratic temperature dependence of the phonon thermal conductivity, is compatible with scattering of phonons that involves either conduction electrons⁴² or tunneling states.⁴³

At low temperatures the relaxation rate of resonant scattering of phonons on tunneling states τ_{TS}^{-1} is proportional to the frequency of the phonon. This $\tau_{\text{TS}}(\omega)$ dependence in the regime where phonon scattering involves tunneling states

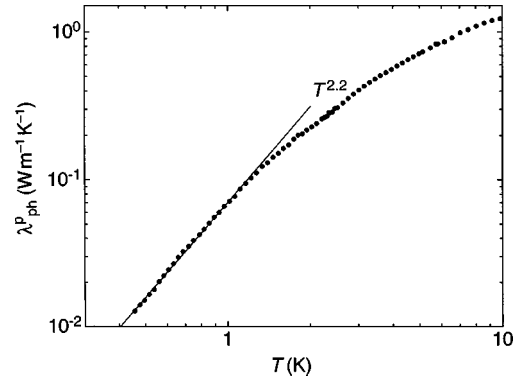


FIG. 10. Phonon contribution λ_{ph}^p as a function of temperature. The solid line indicates a power-law approximation $\lambda_{\text{ph}}^p \propto T^n$ between 0.45 and 1.2 K.

leads to a thermal resistance $\lambda_{\text{ph}}^{-1} \propto T^{-2}$. In icosahedral Al-Mn-Pd and Al-Re-Pd, the presence of tunneling states was identified by measurements of the low-temperature thermal conductivity^{38,41} and by the results of a low-temperature ultrasound experiment which revealed a logarithmic deviation in the sound-velocity variation with temperature and a non-linear attenuation of acoustic shear waves at low temperatures.⁴⁴

The relaxation rate of phonons due to scattering on electrons τ_{pe}^{-1} is also expected to be proportional to the phonon frequency, i.e., $\tau_{\text{pe}}^{-1} \propto \omega$ and hence the corresponding lattice thermal conductivity $\lambda_{\text{ph}}(T)$ is expected to be proportional to T^2 .⁴⁵ Such a $\lambda_{\text{ph}}(T)$ variation has been verified for metallic alloys, for which the lattice contribution λ_{ph} is comparable to the measured thermal conductivity. One example is the lattice conduction in the normal state of single crystals of cadmium-doped tin where a fair agreement between the measured values of λ_{ph} and theoretical calculations was observed.⁴⁶

To conclude our discussion of the mechanism responsible for the thermal resistance of decagonal Al-Ni-Co at low temperatures, we note that the relatively low electrical resistivity $\rho^p(T)$ of decagonal Al-Ni-Co along the periodic direction is of the order of those of d -transition metals and alloys,³ suggesting that a substantial part of the phonon thermal resistance $(\lambda_{\text{ph}}^p)^{-1}$ is due to phonon-electron scattering.

C. Optical conductivity

In Fig. 11 the room temperature reflectivity R of $\text{Al}_{71}\text{Ni}_{16}\text{Co}_{13}$ is plotted as a function of frequency ω on a semilogarithmic scale for both experimental geometries, i.e., for $\mathbf{E} \parallel \mathbf{A}_{10}$ and for $\mathbf{E} \perp \mathbf{A}_{10}$. For comparison, $R(\omega)$ of $\text{Al}_{70}\text{Mn}_9\text{Pd}_{21}$ is also plotted in this figure. Within the accuracy of our experiment, no difference was found between the reflectivity $R(\omega)$ spectrum obtained from the surface parallel to the quasiperiodic plane and the $R(\omega)$ data obtained using linearly polarized light with the electric field \mathbf{E} direction normal to the decagonal axis. Also, no significant temperature dependence of $R(\omega)$ was found. Our $R(\omega)$ results are in general agreement with the first optical measurements on decagonal quasicrystals grown from the $\text{Al}_{62}\text{Co}_{15}\text{Cu}_{20}\text{Si}_3$ and $\text{Al}_{65}\text{Co}_{17}\text{Cu}_{18}$ melts and performed only up to 5 eV.⁷ However, for decagonal Al-Ni-Co the reflectivity spectra reveal

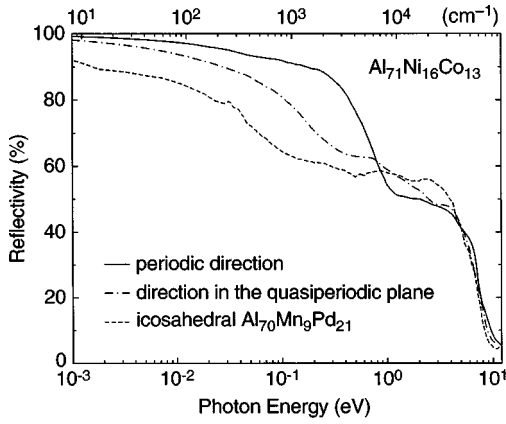


FIG. 11. Reflectivity spectra at 300 K of decagonal $\text{Al}_{71}\text{Ni}_{16}\text{Co}_{13}$ along both polarization directions (i.e., periodic and quasiperiodic) and of icosahedral $\text{Al}_{70}\text{Mn}_9\text{Pd}_{21}$ (from Ref. 13).

only very weak features in the FIR that might be identified as lattice excitations, because those are apparently screened by the more abundant free charge carriers. Also, our $R(\omega)$ data for the periodic direction show a broad FIR feature at ~ 0.1 eV (see below), again quite in contrast to the findings of Ref. 7.

At first sight, our reflectivity spectra displayed in Fig. 11 show a metallic behavior with a plasma-edge-type feature at about 10 eV and the reflectivity $R(\omega)$ approaching 100% for frequencies close to zero frequency. A closer look, however, reveals more complex features, particularly in the form of a broad shoulder in the visible spectral range. We also note that the less conducting icosahedral $\text{Al}_{70}\text{Mn}_9\text{Pd}_{21}$ is characterized by a less intense reflectivity below 0.6 eV, whereas the broad signal in the visible spectral range is more intense (see Fig. 11). Finally, for a quasiperiodic direction of $\text{Al}_{71}\text{Ni}_{16}\text{Co}_{13}$, the onset of electronic interband transitions can be identified above 10 eV.

The optical anisotropy of decagonal $\text{Al}_{71}\text{Ni}_{16}\text{Co}_{13}$ clearly manifests itself in the optical conductivity $\sigma_1(\omega)$ spectra plotted on a semilogarithmic scale in Fig. 12. The difference between $\sigma_1(\omega)$ for the periodic direction and for a direction in the quasiperiodic plane is most prominent in the frequency range below 2 eV. For the periodic direction, $\sigma_1(\omega)$ shows a typical Drude-like component, indicating rather conventional

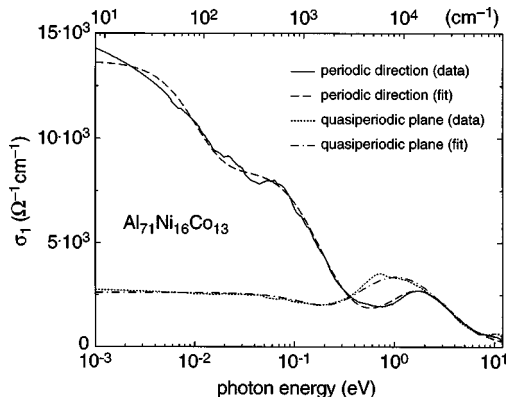


FIG. 12. Real part $\sigma_1(\omega)$ of the optical conductivity at 300 K along both polarization directions. The dashed and dot-dashed lines represent the phenomenological Drude-Lorentz fit (see text).

metallic behavior. One can also identify the already mentioned broad shoulder overlapping with the Drude contribution at 0.1 eV and an absorption at approximately 2 eV. On the other hand, $\sigma_1(\omega)$ in the quasiperiodic plane displays a frequency-independent behavior followed by an onset of a rather broad absorption peaked at about 1 eV. These latter two absorptions in $\sigma_1(\omega)$ at 2 eV in the periodic direction and at 1 eV in the quasiperiodic plane were not clearly resolved in decagonal Al-Cu-Co (Ref. 7) (see below).

In order to better highlight various contributions to the excitation spectrum of $\text{Al}_{71}\text{Ni}_{16}\text{Co}_{13}$, we apply the classical dispersion theory of Lorentz and Drude.⁴⁷ In the quasiperiodic plane, $\sigma_1(\omega)$ can be described by a fairly broad Drude term with a damping $\Gamma \sim 0.2$ eV, a plasma frequency ω_p of about 2 eV, and a harmonic oscillator centered at 1 eV. On the other hand, $\sigma_1(\omega)$ for the periodic direction is dominated by a much more narrow Drude contribution with $\omega_p \sim 1.2$ eV and $\Gamma \sim 1.4 \times 10^{-2}$ eV. While the additional absorption at 2 eV could possibly be assigned to excitations of charge carriers across a pseudogap in the electronic density of states,^{13,14} the origin of the FIR excitation centered at 0.1 eV is, at present, unknown. We note that the total spectral weight of the optical conductivity $\sigma_1(\omega)$ is the same for both polarization directions. This implies that first the anisotropy of the conductivity due to “band structure” effects may be neglected and second, that the anisotropy in $\sigma_1(\omega)$ (Fig. 12) must be attributed to the anisotropy of the scattering rate.⁷ Indeed, the scattering rate Γ for the quasiperiodic plane is more than a factor 10 larger than that along the periodic axis, obviously leading to the fairly flat $\sigma_1(\omega)$ from FIR up to approximately 0.1 eV.

As far as the plasma frequencies ω_p are concerned, we immediately note that they are an order of magnitude larger than those of the less conducting Al-Re-Pd quasicrystals and are comparable to ω_p of icosahedral Al-Mn-Pd.^{11–14} The assumption that the effective mass m^* is close to the free electron mass leads to a concentration of itinerant charge carriers that is at least two orders of magnitude higher than the values previously reported for distinctly less conducting icosahedral quasicrystals.^{11–14}

A rough estimate of the effective mass m^* and the concentration n of the itinerant charge carriers may be obtained from a direct comparison of the plasma frequency ω_p , associated with the metallic Drude contribution to $\sigma_1(\omega)$, with the value of the linear term γ in the low-temperature specific heat. In doing so we have to keep in mind that γ is proportional to the average density of electronic states at E_F for all directions and therefore our calculation may only serve as setting a trend. Using $\gamma = 0.629$ mJ mol⁻¹ K⁻² (see Sec. III A) and $\omega_p \approx 2$ eV we obtain $n \approx 7.3 \times 10^{21}$ cm⁻³ and $m^*/m_e \approx 2.5$ in the quasiperiodic plane and with $\omega_p \approx 1.2$ eV we obtain $n \approx 3.4 \times 10^{21}$ cm⁻³ and $m^*/m_e \approx 3.9$ for the periodic direction. While these values of n are in fair agreement with the charge-carrier concentration estimated from the results of Hall effect measurements,²⁷ they are exceedingly lower than the estimate based upon the atomic density and the effective valency of the constituent elements.²⁷ Once again this confirms the presence of a pseudogap in the density of electronic states at E_F .

In Fig. 13 the optical conductivity $\sigma_1(\omega)$ of $\text{Al}_{71}\text{Ni}_{16}\text{Co}_{13}$ is plotted on double logarithmic scales. Also shown in that

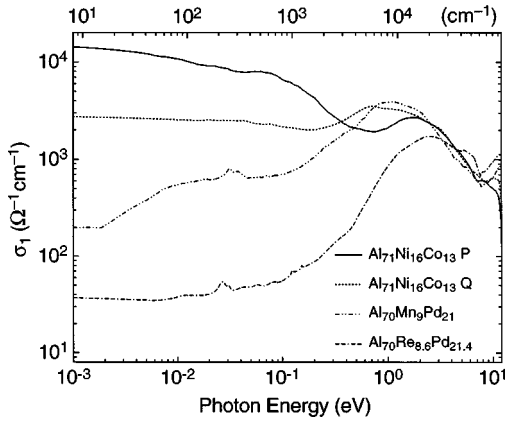


FIG. 13. $\sigma_1(\omega)$ of the decagonal $\text{Al}_{71}\text{Ni}_{16}\text{Co}_{13}$ at 300 K along the periodic direction (P) and along a direction in the quasiperiodic plane (Q) in comparison with icosahedral $\text{Al}_{70}\text{Mn}_9\text{Pd}_{21}$ (Ref. 13) and $\text{Al}_{70}\text{Re}_{8.6}\text{Pd}_{21.4}$ (Ref. 14).

figure are the $\sigma_1(\omega)$ spectra of two icosahedral quasicrystals— $\text{Al}_{70}\text{Mn}_9\text{Pd}_{21}$ (Ref. 13) and $\text{Al}_{70}\text{Re}_{8.6}\text{Pd}_{21.4}$.¹⁴ As a first observation we note that in the FIR and up to the MIR spectral range, $\sigma_1(\omega)$ of icosahedral quasicrystals tends to slowly increase with increasing frequency, i.e., quite in contrast with the frequency-independent behavior in the quasiperiodic plane of decagonal $\text{Al}_{71}\text{Ni}_{16}\text{Co}_{13}$ that is characteristic of disordered or amorphous metals. Also, the values of $\sigma_1(\omega)$ in the quasiperiodic plane in the low-frequency limit is typical rather of amorphous metals than of highly ordered icosahedral quasicrystals with dc conductivity values that are below the Mott minimum metallic conductivity.^{11–14}

The most striking difference between the optical conductivity spectra of decagonal and icosahedral quasicrystals is, however, the less prominent pseudogap feature in the $\sigma_1(\omega)$ spectra of the decagonal quasicrystals. In decagonal Al-Ni-Co the absorptions visible in $\sigma_1(\omega)$ at 1 eV along a direction in the quasiperiodic plane and at 2 eV along the periodic direction can be attributed to a pseudogap in the electronic DOS and electronic interband transitions, respectively. Such absorptions in $\sigma_1(\omega)$, although with less intensity, were previously observed in decagonal Al-Cu-Co.⁷ This difference in the intensities of these absorptions between Al-Ni-Co and Al-Cu-Co most likely originates in the $R(\omega)$ data available for the Kramers-Kronig transformation which for Al-Cu-Co (Ref. 7) extends up to a lower high-frequency limit and consequently affects $\sigma_1(\omega)$. We recall that a well-developed pseudogap that seems to be characteristic of icosahedrally structured solids has been associated with the Hume-Rothery-type stabilization mechanism. In our previous investigations of the complete electrodynamic response of icosahedral quasicrystals, we recognized a shift of the pseudogap from the weakly conducting Re-based quasicrystals towards lower frequencies for more conducting Mn-based quasicrystals.^{13,14} For decagonal quasicrystals the gap frequency is further reduced which, together with the still higher conductivity substantially screens the pseudogap feature. This difference between the optical conductivity spectra of icosahedral and decagonal quasicrystals would support the scenario, in which the major difference between the two families is the difference in the density of free charge carriers

and consequently quite different spectral weights in the corresponding Drude contributions to $\sigma_1(\omega)$.

IV. SUMMARY AND CONCLUSIONS

The specific heat $C_p(T)$ and both components of the thermal conductivity tensor $\lambda^p(T)$ and $\lambda^q(T)$ of decagonal Al-Ni-Co were measured in varying temperature ranges between 0.06 and 80 K. The optical conductivities along the periodic $\sigma_1^p(\omega)$ and the quasiperiodic direction $\sigma_1^q(\omega)$ were determined from the analysis of the reflectivity $R(\omega)$ measurements in the frequency range between 0.1 meV and 12 eV using linearly polarized light.

Below 3 K, the specific heat can adequately be described as the sum of a linear-in- T term and a cubic-in- T term, i.e., assuming that $C_p(T)$ is due to electronic and lattice excitations. The coefficient γ of the linear term in the specific heat amounts to about one third of the γ value of aluminum indicating that the density of electronic states at E_F is reduced. The cubic-in- T term in $C_p(T)$ agrees well with the contribution of the long wavelength acoustic excitations calculated using low-temperature values of the elastic moduli c_{ij} obtained for this same sample.¹⁸ We did not find any indications for an excess specific heat, contrary to what has previously been observed in icosahedral Al-Mn-Pd and Al-Re-Pd.³³ Above 3 K, the lattice specific heat $C_{\text{ph}} = C_p - \gamma T$ increases with increasing temperature more steeply than T^3 . The deviation $C_{\text{ph}} - \beta T^3$ between the experimentally determined lattice specific heat and the Debye-type expectations varies approximately as T^5 . A term in the lattice specific heat C_{ph} that varies as T^5 may originate from the dispersion of acoustic excitations. However, the $\omega(\mathbf{q})$ data for decagonal Al-Ni-Co as determined from the results of inelastic neutron scattering experiments³⁵ cannot account for the magnitude of the T^5 term in the specific heat.

The phonon thermal conductivity $\lambda_{\text{ph}}^q(T)$ along a direction in the quasiperiodic plane is distinctly different from that along the periodic direction $\lambda_{\text{ph}}^p(T)$. Between 30 and 70 K, $\lambda_{\text{ph}}^q(T)$ is weakly temperature dependent. This feature of the $\lambda_{\text{ph}}^q(T)$ curve was previously observed for decagonal Al-Cu-Co (Ref. 5) as well as for icosahedral quasicrystals^{38–41} and has been attributed to generalized Umklapp scattering of phonons in quasicrystals.⁹ The phonon thermal conductivity along the periodic direction $\lambda_{\text{ph}}^p(T)$ is characterized by a distinct maximum at 25 K, which can be attributed to a crossover between the Peierls regime of the usual Umklapp phonon scattering⁸ and the regime of phonon-electron scattering. This $\lambda_{\text{ph}}^p(T)$ behavior is reminiscent of $\lambda_{\text{ph}}(T)$ of periodic crystals. Thus, the transport of heat via lattice excitations along the decagonal axis and along a direction in the quasiperiodic plane resembles closely that of periodic crystals and icosahedral quasicrystals, respectively. Surprisingly, the lattice thermal conductivity in decagonal Al-Ni-Co is higher along a direction in the quasiperiodic plane, than along the periodic direction. The inequality $\lambda_{\text{ph}}^q > \lambda_{\text{ph}}^p$ seems to be a general observation for decagonal quasicrystals⁵ and is possibly related to strongly anisotropic phonon-electron scattering.

The optical reflectivity $R(\omega)$ of decagonal Al-Ni-Co also shows a strongly anisotropic behavior. For the periodic direction, $\sigma_1^p(\omega)$ is dominated at low frequencies by a narrow Drude contribution with a plasma frequency $\omega_p \sim 1.2$ eV and a scattering rate Γ of the free charge carriers $\Gamma \sim 1.4 \times 10^{-2}$ eV and two additional absorptions centered at 0.1 eV and at 2 eV at higher frequencies. The optical conductivity along the quasiperiodic direction $\sigma_1^q(\omega)$ is characterized by a much broader Drude contribution with $\omega_p \sim 2$ eV and $\Gamma \sim 0.2$ eV and only one high-frequency absorption centered at 1 eV. These absorptions at 2 and 1 eV for the periodic direction and a direction in the quasiperiodic plane, respectively, are possibly related to a pseudogap-like absorption. It is particularly interesting that these absorptions are less pronounced in the case of decagonal quasicrystals compared to the icosahedral quasicrystals, which is due to the higher conductivity of decagonal quasicrystals at low frequencies. A direct comparison of $\omega_p \approx 2$ eV obtained along the quasiperiodic direction and the linear-in- T term to the specific heat

$\gamma = 0.629$ mJ mol $^{-1}$ K $^{-2}$ yields a charge carrier concentration $n \approx 7.3 \times 10^{21}$ cm $^{-3}$ and an effective mass ratio $m^*/m_e \approx 2.5$.

ACKNOWLEDGMENTS

We thank S. Ritsch and H.-J. Schwer for their help in the electron microscopy and the x-ray characterization of our samples and J. Müller for technical assistance. We are grateful to M. de Boissieu and F. Dugain for supplying us with the phonon dispersion data of decagonal Al-Ni-Co prior to publication. F. B. and L. D. would like to thank P. Wachter for his generous support in providing infrastructures related to these experiments. This work was in part supported by the Schweizerische Nationalfonds zur Förderung der wissenschaftlichen Forschung. K. E. acknowledges the financial support from the Ministry of Education, Science, and Culture of Japan.

- ¹B. Grushko and K. Urban, *Philos. Mag.* B **70**, 1063 (1994); K. Edagawa, H. Tamaru, S. Yamaguchi, K. Suzuki, and S. Takeuchi, *Phys. Rev. B* **50**, 12 413 (1994); T. Gödecke, *Z. Metallkd.* **88**, 557 (1997); T. Gödecke, M. Scheffer, R. Lück, S. Ritsch, and C. Beeli, *ibid.* **88**, 687 (1997), and references therein.
- ²S. Lin, X. Wang, L. Lu, D. Zhang, L. X. He, and K. X. Kuo, *Phys. Rev. B* **41**, 9625 (1990).
- ³T. Shibuya, T. Hashimoto, and S. Takeuchi, *J. Phys. Soc. Jpn.* **59**, 1917 (1990).
- ⁴Dian-Lin Zhang, Shao-Chun Cao, Yun-Ping Wang, Li Lu, Xue-Mei Wang, X. L. Ma, and K. H. Kuo, *Phys. Rev. Lett.* **66**, 2778 (1991).
- ⁵K. Edagawa, M. A. Chernikov, A. D. Bianchi, E. Felder, U. Gubler, and H. R. Ott, *Phys. Rev. Lett.* **77**, 1071 (1996).
- ⁶D. G. Naugle, W. D. Bruton, K. D. D. Rathnayaka, and A. R. Kortan, *J. Non-Cryst. Solids* **205-207**, 17 (1996).
- ⁷D. N. Basov, T. Timusk, F. Barakat, J. Greedan, and B. Grushko, *Phys. Rev. Lett.* **72**, 1937 (1994).
- ⁸R. Peierls, *Ann. Phys. (Leipzig)* **3**, 1055 (1929).
- ⁹P. A. Kalugin, M. A. Chernikov, A. Bianchi, and H. R. Ott, *Phys. Rev. B* **53**, 14 145 (1996).
- ¹⁰J. Hafner, M. Krajčí, and M. Mihalkovič, *Phys. Rev. Lett.* **76**, 2738 (1996).
- ¹¹C. C. Homes, T. Timusk, X. Wu, Z. Altounian, A. Sahnoun, and J. O. Ström-Olsen, *Phys. Rev. Lett.* **67**, 2694 (1991).
- ¹²D. N. Basov, F. S. Pierce, P. Volkov, S. J. Poon, and T. Timusk, *Phys. Rev. Lett.* **73**, 1865 (1994).
- ¹³L. Degiorgi, M. A. Chernikov, C. Beeli, and H. R. Ott, *Solid State Commun.* **87**, 721 (1993).
- ¹⁴A. D. Bianchi, F. Bommeli, M. A. Chernikov, U. Gubler, L. Degiorgi, and H. R. Ott, *Phys. Rev. B* **55**, 5730 (1997).
- ¹⁵A. M. Karo and J. R. Hardy, *Phys. Rev.* **129**, 2024 (1963); R. A. Cowley, W. Cochran, B. N. Brockhouse, and A. D. B. Woods, *ibid.* **131**, 1030 (1963).
- ¹⁶U. Mizutani, T. Matsuda, Y. Itoh, K. Tanaka, H. Domae, T. Mizuno, S. Murasaki, Y. Miyoshi, K. Hashimoto, and Y. Yamada, *J. Non-Cryst. Solids* **156-158**, 882 (1993).
- ¹⁷S. Ritsch, Ph.D. thesis, ETH, Zürich, 1996.
- ¹⁸M. A. Chernikov, H. R. Ott, A. Bianchi, A. Migliori, and T. W. Darling, *Phys. Rev. Lett.* **80**, 321 (1998).
- ¹⁹M. A. Chernikov, A. Bernasconi, C. Beeli, A. Schilling, and H. R. Ott, *Phys. Rev. B* **48**, 3058 (1993).
- ²⁰Z. M. Stadnik, D. Purdie, M. Garnier, Y. Baer, A. P. Tsai, A. Inoue, K. Edagawa, and S. Takeuchi, *Phys. Rev. Lett.* **77**, 1777 (1996). In this work the photoelectron spectra which, strictly speaking, do not show the pseudogap at E_F directly, were analyzed assuming that the electronic DOS can adequately be represented by a superposition of a pseudogap of Lorentzian shape centered at E_F and a linearly varying DOS in the vicinity of E_F . The background contribution was determined using a linear extrapolation of the data taken in the energy range between -1.2 and -0.7 eV. The data analysis yielded a width of the pseudogap between 0.22 and 0.36 eV with a relative reduction of the density of electronic states in the range from 28 to 61 %.
- ²¹G. T. de Laissardière and T. Fujiwara, *Phys. Rev. B* **50**, 5999 (1994).
- ²²M. Krajčí, M. Windisch, J. Hafner, G. Kresse, and M. Mihalkovič, *Phys. Rev. B* **51**, 17 355 (1995).
- ²³G. T. de Laissardière, D. N. Manh, L. Magaud, J. P. Julien, F. Cyrot-Lackmann, and D. Mayou, *Phys. Rev. B* **52**, 7920 (1995).
- ²⁴J. Friedel, *Helv. Phys. Acta* **61**, 538 (1988).
- ²⁵K. Kimura and S. Takeuchi, in *Quasicrystals: The State of the Art*, edited by D. DiVincenzo and P. Steinhardt (World Scientific, Singapore, 1991); S. J. Poon, *Adv. Phys.* **41**, 303 (1992), and references therein.
- ²⁶P. A. Bancel and P. A. Heiney, *Phys. Rev. B* **33**, 7917 (1986).
- ²⁷Y. Wang, D. Zhang, and L. F. Chen, *Phys. Rev. B* **48**, 10 542 (1993).
- ²⁸Z. M. Stadnik, D. Purdie, M. Garnier, Y. Baer, A. P. Tsai, A. Inoue, K. Edagawa, S. Takeuchi, and K. H. J. Buschow, *Phys. Rev. B* **55**, 10 938 (1997). In this work the experimentally determined photoemission intensity in the energy range between -2.0 and -1.5 eV and from -2.2 to -1.8 eV, for Al-Cu-Co and Al-Ni-Co, respectively, was linearly extrapolated. An analysis of the photoemission spectra, assuming the DOS in the form of a Lorentzian pseudogap at E_F superimposed on a linear term,

- is consistent with a pseudogap that is wider, i.e., between 0.9 and 1.1 eV, but deeper (80–85 %) than in icosahedral quasicrystals (Ref. 20). We note, however, that similarly to what was reported for icosahedral phases (Ref. 20), the as-measured photoelectron emission spectra do not display a pseudogap at the Fermi energy E_F .
- ²⁹R. F. Sabiryanov, S. K. Bose, and S. E. Burkov, *J. Phys.: Condens. Matter* **7**, 5437 (1995).
- ³⁰M. Krajčí, J. Hafner, and M. Mihalkovič, *Phys. Rev. B* **56**, 3072 (1997).
- ³¹G. T. de Laissardière and T. Fujiwara, *Phys. Rev. B* **50**, 9843 (1994).
- ³²M. Krajčí, J. Hafner, and M. Mihalkovič, *Europhys. Lett.* **34**, 207 (1996); *Phys. Rev. B* **55**, 843 (1997).
- ³³C. Wälti, E. Felder, M. A. Chernikov, H. R. Ott, M. de Boissieu, and C. Janot, *Phys. Rev. B* **57**, 10 504 (1998).
- ³⁴I. M. Lifshitz, *Zh. Eksp. Teor. Fiz.* **26**, 551 (1954).
- ³⁵F. Dugain, M. de Boissieu, K. Hradil, K. Shibata, R. Currat, A. R. Kortan, A. P. Tsai, J.-B. Suck, and F. Frey, in *Aperiodic'97: International Conference on Aperiodic Crystals*, Alpe d'Huez, France, 1997, edited by M. de Boissieu, R. Currat, and J.-L. Verger-Gaugry (World Scientific, Singapore, 1998).
- ³⁶C. L. Henley, *J. Non-Cryst. Solids* **153-154**, 172 (1993).
- ³⁷M. Mihalkovič, F. Dugain, and J.-B. Suck, *J. Non-Cryst. Solids* **205-207**, 701 (1996).
- ³⁸M. A. Chernikov, A. Bianchi, and H. R. Ott, *Phys. Rev. B* **51**, 153 (1995).
- ³⁹A. Perrot, J.-M. Dubois, M. Cassart, and J. P. Issi, in *Quasicrystals*, Proceedings of the 5th International Conference, Avignon, France, 1995, edited by C. Janot and R. Mosseri (World Scientific, Singapore, 1995), p. 588.
- ⁴⁰S. Legault, B. Ellman, J. Ström-Olsen, L. Taillefer, and S. Kycia, in *Quasicrystals* (Ref. 39), p. 592.
- ⁴¹M. A. Chernikov, A. D. Bianchi, E. Felder, U. Gubler, and H. R. Ott, *Europhys. Lett.* **35**, 431 (1996).
- ⁴²R. Berman, *Thermal Conduction in Solids* (Clarendon, Oxford, 1976).
- ⁴³W. A. Phillips, *J. Low Temp. Phys.* **7**, 351 (1972); P. W. Anderson, B. I. Halperin, and C. M. Varma, *Philos. Mag.* **25**, 1 (1972).
- ⁴⁴N. Vernier, G. Bellessa, B. Perrin, A. Zarembowitch, and M. de Boissieu, *Europhys. Lett.* **22**, 187 (1993).
- ⁴⁵P. G. Klemens, in *Kältephysik I*, Vol. XIV of *Handbuch der Physik*, edited by S. Flügge (Springer, Berlin, 1956), p. 198.
- ⁴⁶M. C. Karamargin, C. A. Reynolds, F. P. Lipschultz, and P. G. Klemens, *Phys. Rev. B* **10**, 3624 (1972).
- ⁴⁷F. Wooten, *Optical Properties of Solids* (Academic, New York, 1972).